

# Cytoplasmic Inclusion Bodies Are Detected by Synthetic Antibody in Ciliated Bronchial Epithelium during Acute Kawasaki Disease

Anne H. Rowley,<sup>1,2</sup> Susan C. Baker,<sup>4</sup> Stanford T. Shulman,<sup>1</sup> Linda M. Fox,<sup>5</sup> Kei Takahashi,<sup>7</sup> Francesca L. Garcia,<sup>1</sup> Susan E. Crawford,<sup>3</sup> Pauline Chou,<sup>3</sup> and Jan M. Orenstein<sup>6</sup>

Departments of <sup>1</sup>Pediatrics, <sup>2</sup>Microbiology/Immunology, and <sup>3</sup>Pathology, Feinberg School of Medicine, Children's Memorial Hospital, Northwestern University, Chicago, and Departments of <sup>4</sup>Microbiology/Immunology and <sup>5</sup>Pathology, Stritch School of Medicine, Loyola University, Maywood, Illinois; <sup>6</sup>Department of Pathology, George Washington University School of Medicine, Washington, DC; <sup>7</sup>Department of Pathology, Toho University School of Medicine, Tokyo, Japan

**Background.** In developed nations, Kawasaki disease (KD) is the most common cause of acquired heart disease in children. An infectious etiology is likely but has not yet been identified. We have previously reported that oligoclonal immunoglobulin A plasma cells infiltrate acute KD tissues and that synthetic KD antibodies detect a distinctive spheroidal antigen in acute KD ciliated bronchial epithelium.

**Methods.** To further characterize the antigen in acute KD bronchi, we examined paraffin-embedded ciliated bronchial epithelium using light microscopy (LM) and transmission electron microscopy (TEM).

**Results.** The spheroids observed by immunohistochemistry (IHC) are visualized as inclusion bodies with hematoxylin-eosin and nucleic acid stains and in methylene blue/azure II/basic fuchsin trichrome-stained plastic sections, suggesting the presence of both protein and nucleic acid. The structures visualized by LM correspond to homogeneous electron-dense perinuclear inclusion bodies (up to 1.4 microns in diameter) in ciliated bronchial epithelium from 4 patients with acute KD examined by TEM. Inclusion bodies were not present in control bronchial epithelium or in nonciliated cells.

**Conclusions.** The antigen detected in acute KD ciliated bronchial epithelium by IHC with synthetic KD antibodies resides in cytoplasmic inclusion bodies that are consistent with aggregates of viral proteins and associated nucleic acid and may derive from the etiologic agent of KD.

Kawasaki disease (KD) is an acute systemic inflammatory illness of early childhood that particularly affects medium-sized arteries, such as the coronary arteries, and that can result in myocardial infarction, coronary artery aneurysms that rupture, and sudden

death [1]. In developed nations, KD has replaced acute rheumatic fever as the most common cause of acquired heart disease in children [2]. Although the etiology is unknown, clinical and epidemiologic data support infection with a ubiquitous microbial agent. This theory predicts that most individuals are asymptotically infected with the agent during childhood and that only a very small subset of genetically predisposed individuals develop clinical features of KD. In this model, the rarity of KD in infants <3 months old is explained by protective, passive maternal antibodies. The rarity of KD in adults is consistent with widespread immunity. Attempts to identify the etiologic agent of KD by traditional methods have not been successful.

Our laboratory has taken an immunologic approach to the investigation of the etiology of KD. We have discovered that IgA plasma cells infiltrate coronary arteries [3] and other inflamed tissues during acute KD [4] and that, compared with control subjects, peribronchial IgA

Received 20 May 2005; accepted 1 July 2005; electronically published 17 October 2005.

Presented in part: 42nd annual meeting of the Infectious Diseases Society of America, Boston, 30 September–3 October 2004 (abstract 105); 8th International Kawasaki Disease Symposium, San Diego, 17–20 February 2005 (abstract 7); 43rd annual meeting of the Infectious Diseases Society of America, San Francisco, 6–9 October 2005 (abstract 56).

Potential conflicts of interest: none reported.

Financial support: National Institutes of Health (grants K02 HL67011 and R01 HL63771 to A.H.R.); Kawasaki Disease Research Fund of Children's Memorial Hospital.

Reprints or correspondence: Dr. Anne H. Rowley, Professor of Pediatrics and of Microbiology/Immunology, Pediatrics W140, Ward 12-204, 303 E. Chicago Ave., Chicago, IL 60611 (a-rowley@northwestern.edu).

**The Journal of Infectious Diseases** 2005;192:1757–66

© 2005 by the Infectious Diseases Society of America. All rights reserved.  
0022-1899/2005/19210-0013\$15.00

plasma cells are significantly increased in the upper respiratory tracts of patients with acute KD, which is similar to findings in children with fatal viral respiratory infections [4]. We have also reported that macrophages and CD8 T lymphocytes are prominent in the inflammatory infiltrate [5]. These immunologic findings suggest the presence of an intracellular pathogen with a respiratory portal of entry.

IgA genes in arteries from patients with acute fatal KD are oligoclonal, that is, are antigen driven [6]. We previously made oligoclonal KD antibodies in vitro and performed immunohistochemical experiments on formalin-fixed, paraffin-embedded tissues from patients with acute KD and from control subjects, and we reported that synthetic KD antibody A identified antigen in acute KD, but not in control, bronchial epithelium as well as in a subset of macrophages in inflamed acute KD tissues, such as the coronary arteries [7]. Antigen was localized to distinctive perinuclear, primarily apical intracytoplasmic “spheroidal bodies” in acute KD ciliated bronchial epithelium by use of synthetic KD antibody A. To further characterize this antigen in acute KD bronchi, we here examine ciliated bronchial epithelium from patients with acute KD by light microscopy (LM) and transmission electron microscopy (TEM).

## PATIENTS, MATERIALS, AND METHODS

**Patients and specimens.** Formalin-fixed, paraffin-embedded lung tissues from patients with fatal acute KD were studied by TEM, because fresh tissue from KD fatalities has been virtually unavailable. Autopsy revealed that patients 1–5 and 7 had coronary artery aneurysms and that patients 8 and 9 had coronary arteritis without aneurysms. Patient 6 had leukemia and developed classic clinical symptoms of acute KD. He developed fatal candidal sepsis 10 days after the onset of KD; autopsy did not reveal evidence of coronary arteritis (table 1). Patients 1, 5, and 7 were included in our previous immunohistochemical study using synthetic KD antibody A [7], as is noted in table 1. Control tissues included formalin-fixed, paraffin-embedded

lung tissue from a 3-month-old infant with respiratory syncytial virus (RSV) infection and from a 12-month-old infant with rotavirus infection. We also studied glutaraldehyde-fixed lung tissue from a 1-month-old infant with congenital heart disease and bronchopneumonia and compared the results with those for formalin-fixed, paraffin-embedded lung tissue from the same patient. The present study was approved by the Institutional Review Board of Children’s Memorial Hospital.

**Synthetic KD antibodies.** Synthetic KD antibodies were made as described elsewhere [7]. Immunohistochemistry (IHC) was performed with synthetic antibodies A and J. Antibody J, made from heavy chain 11-5 [6] and light chain 9-8 [7], was prepared after our initial synthetic antibody study and demonstrates strong binding to acute KD ciliated bronchial epithelium. Control synthetic antibody I, made from heavy chain 4-2 [6] and light chain 9-8 [7], does not demonstrate binding to acute KD or control ciliated bronchial epithelium.

**IHC.** Formalin-fixed, paraffin-embedded tissue sections were deparaffinized by use of xylene, rehydrated, and heated in 10 mmol/L sodium citrate buffer (pH 6.0), to enhance antigen retrieval, as described elsewhere [7]. Sections were incubated with 10–50 µg/mL biotinylated synthetic antibody A, J, or I, and color was developed by use of the Vectastain Elite ABC Kit (Vector). Diaminobenzidine tetrahydrochloride was used as a reaction product, to generate a brown stain. Sections were lightly counterstained with hematoxylin. We recorded positive results when strong brown staining of intracytoplasmic bodies was observed in ciliated bronchial epithelial cells.

**Hematoxylin-eosin (HE), Feulgen, methyl green pyronin (MGP), and Fontana stains.** Standard HE, Feulgen, MGP, and Fontana staining was also performed on formalin-fixed, paraffin-embedded lung tissue.

**TEM.** TEM was performed in 2 different laboratories. At Loyola University, resin blocks were made from tissue sections from patients 1, 3, and 4 after IHC with synthetic antibody, to

**Table 1. Patients with Kawasaki disease (KD) included in the present study.**

Patient (sex, age)	Included in previous study <sup>a</sup> [7]	Ethnicity	Duration of illness before death	Treatment	Cause of death	Year of death
1 (M, 4 months)	Yes (KD7)	White	3 weeks	IVGG, aspirin	Myocarditis	2000
2 (M, 7 months)	No	White	4 weeks	Aspirin	Myocardial infarction	1982
3 (M, 9 months)	No	Unknown	8 weeks	Prednisone	Myocardial infarction	1978
4 (M, 9 months)	No	Japanese	18 days	IVGG, aspirin	Myocardial infarction	1991
5 (M, 6 months)	Yes (KD1)	White	5 weeks	IVHC	Myocardial infarction	1974
6 (M, 6 years)	No	Japanese	10 days	None	Leukemia, candidal sepsis	1981
7 (F, 10 months)	Yes (KD13)	Black	5 weeks	Aspirin	Myocardial infarction	1984
8 (M, 5 years)	No	Japanese	6 days	Aspirin	Myocarditis	1970
9 (F, 19 months)	No	Japanese	29 days	Aspirin	Interstitial pneumonia	1979

**NOTE.** IVGG, intravenous gammaglobulin; IVHC, intravenous hydrocortisone.

<sup>a</sup> Shown in parentheses are the patient identification nos. from the previous study.

allow for accurate localization of bronchi containing the spheroidal bodies within the lung section. Tissue sections were treated with osmium tetroxide, dehydrated in graded ethanol, and transitioned through propylene oxide into increasing concentrations of epoxy resin. A prepolymerized blank epoxy block was positioned over the area of interest, and the slide was placed into a 60°C oven overnight. The block was snapped off the glass slide after brief contact with dry ice or quick immersion in liquid nitrogen, or both. The block was aligned and thin-sectioned immediately at 80 nm by use of a diamond knife. Sections were picked up on fine bar grids and stained with uranyl acetate and lead citrate, and the grids were viewed on a Hitachi H600 transmission electron microscope at 75 kV.

At George Washington University, pieces of formalin-fixed, paraffin-embedded lung tissue (patient 2) were excised directly from areas of a tissue block containing bronchi that were positive by IHC. The paraffin-embedded tissue was placed on filter paper and warmed to 60°C for 5 min, to remove excess paraffin. To remove the remaining paraffin, the tissue was processed through xylene and decreasing ethanol concentrations and was brought to aqueous PBS neutral buffer. The tissue was then postfixed in osmium tetroxide, processed through graded ethanol and propylene oxide, and embedded in Spurr's epoxy. Semithin (1 micron) plastic sections were cut by use of a glass knife and were stained with the methylene blue/azure II/basic fuchsin trichrome stain for plastic-section LM. The blocks selected for TEM were thinned by use of a diamond knife, stained with uranyl acetate and lead citrate, and examined on a LEO EM10 transmission electron microscope operating at 60 kV.

## RESULTS

We noted remarkable similarity between the LM appearance of the KD structures observed by IHC with synthetic KD antibody and intracytoplasmic inclusion bodies of various RNA viruses, such as members of the *Paramyxoviridae* family [8]. We used LM stains and TEM to determine whether intracytoplasmic inclusion bodies were present in acute KD bronchial epithelium and to determine whether, in addition to protein, nucleic acid was a component of the bodies (table 2).

**IHC.** Dark brown-staining (mostly supranuclear) intracytoplasmic bodies were observed in ciliated epithelial cells of medium-sized bronchi from patients 1–6, 8, and 9 (figures 1 and 2) with synthetic antibodies A and J; these were not observed with control synthetic antibody I. Large bronchi (completely encased by cartilage) and small, nonciliated bronchi generally did not stain with synthetic antibodies A or J. All tissues that were positive with synthetic antibody A were also positive with synthetic antibody J and had the same pattern of staining, although antibody J generally resulted in stronger staining than did antibody A. Ciliated bronchial epithelium from patient 7 did not stain with synthetic antibody A or J, nor did bronchial epitheli-

um from the control subjects. Nonciliated goblet cells (in the same acute KD bronchi in which positive ciliated cells were present) were also negative, as were control bronchi. Although most IHC-positive bronchi showed no evidence of cellular cytotoxicity [7], some bronchi (from patients 4 and 8) did demonstrate acute bronchitis and even necrotizing bronchitis (figure 2). For patient 4, the preserved epithelial cells in damaged bronchi contained antigen (figure 2).

**HE.** Relatively subtle, round to oval intracytoplasmic perinuclear inclusion bodies could be observed in medium-sized bronchi from patients 1, 2, 4–6, 8, and 9 when stained with HE and examined by LM (figure 1). The inclusion bodies often were amphophilic (staining with both eosin and hematoxylin), suggesting that they contained both protein and nucleic acid. No inclusion bodies were observed for patients 3 and 7 or in control bronchial epithelium.

**Fontana stains for lipofuscin.** Close analysis of HE-stained sections of bronchial epithelium from several patients with acute KD (patients 4–6) revealed the presence of irregular, golden yellow, granular supranuclear pigment resembling classic lipofuscin in ciliated bronchial epithelial cells (figure 1). Furthermore, in addition to the typical spheroidal bodies, IHC revealed pleomorphic, supranuclear, dark brown-staining material with synthetic antibodies A and J (figures 1 and 2) but not with control synthetic antibody I, suggesting that the antibody was also staining lipofuscin bodies. Therefore, we also performed Fontana staining for lipofuscin. For patients 3, 5, and 6, typical black, supranuclear, granular, lipofuscin staining of the ciliated epithelial cells was observed. However, the level of Fontana staining was much less than the amount of golden yellow granular pigment observed by HE staining and the pleomorphic material stained by IHC. This indicated that the Fontana stain was staining only a relatively small portion of what appeared to be classic lipofuscin in HE sections and suggested that the material that resembled lipofuscin but that was not detected by Fontana stain was KD antigen revealed by IHC. Fontana staining was negative for patients 4 and 7 and in control bronchial epithelium.

**Feulgen and MGP stains.** On the basis of staining of other cells that can serve as an internal control, the color balance of both the Feulgen and MGP stains appeared to be suboptimal. Nevertheless, the stains clearly delineated the inclusion bodies, indicating that they likely contained nucleic acid. However, because of the suboptimal staining, it was not possible to determine whether the nucleic acid was RNA or DNA. This could have resulted from prolonged initial formalin fixation and/or fixation under acid conditions.

**Semithin plastic sections.** Perinuclear inclusion bodies were observed in semithin plastic sections from the only patient (patient 2) for whom tissue was retrieved from a paraffin block for TEM. They appeared dark blue with the methylene blue/azure

**Table 2. Results of experiments with acute Kawasaki disease (KD) ciliated bronchial epithelial cells.**

Patient	IHC with synthetic KD antibody	Stain				
		HE	Fontana <sup>a</sup>	Feulgen	MGP	TEM
1	Positive	ICI	ND	ND	ND	ICI (IHC and TEM show bodies in same location in cell)
2	Positive	ICI, shedding of bronchial epithelium	ND	ND	ICI	Rare ICI (STPS also shows ICI [dark blue])
3	Positive (veins, alveolar septal cells, and interstitial macrophages also positive)	Normal appearance	Positive	Negative	Negative	ICI (ICI also present in interstitial cells)
4	Positive	ICI, LF, necrotizing bronchitis	Negative	ICI	ICI	Rich in electron-dense bodies of various sizes, including ICI
5	Positive	LF, shedding of bronchial epithelial cells	Positive	Rare ICI	Negative	ND
6	Positive	ICI, LF	Positive	ICI	ICI	ND
7	Negative	Bronchitis	Negative	Negative	ND	ND
8	Positive	ICI, bronchitis	ND	ND	ND	ND
9	Positive	ICI	ND	ND	ND	ND

**NOTE.** HE, hematoxylin-eosin; ICI, intracytoplasmic inclusion bodies; IHC, immunohistochemistry; LF, lipofuscin (golden yellow granular pigment); MGP, methyl green pyronin; ND, not done; STPS, semithin plastic sections (methylene blue/lazure II/basic fuchsin trichrome stain); TEM, transmission electron microscopy.

<sup>a</sup> Fontana is a stain for lipofuscin.

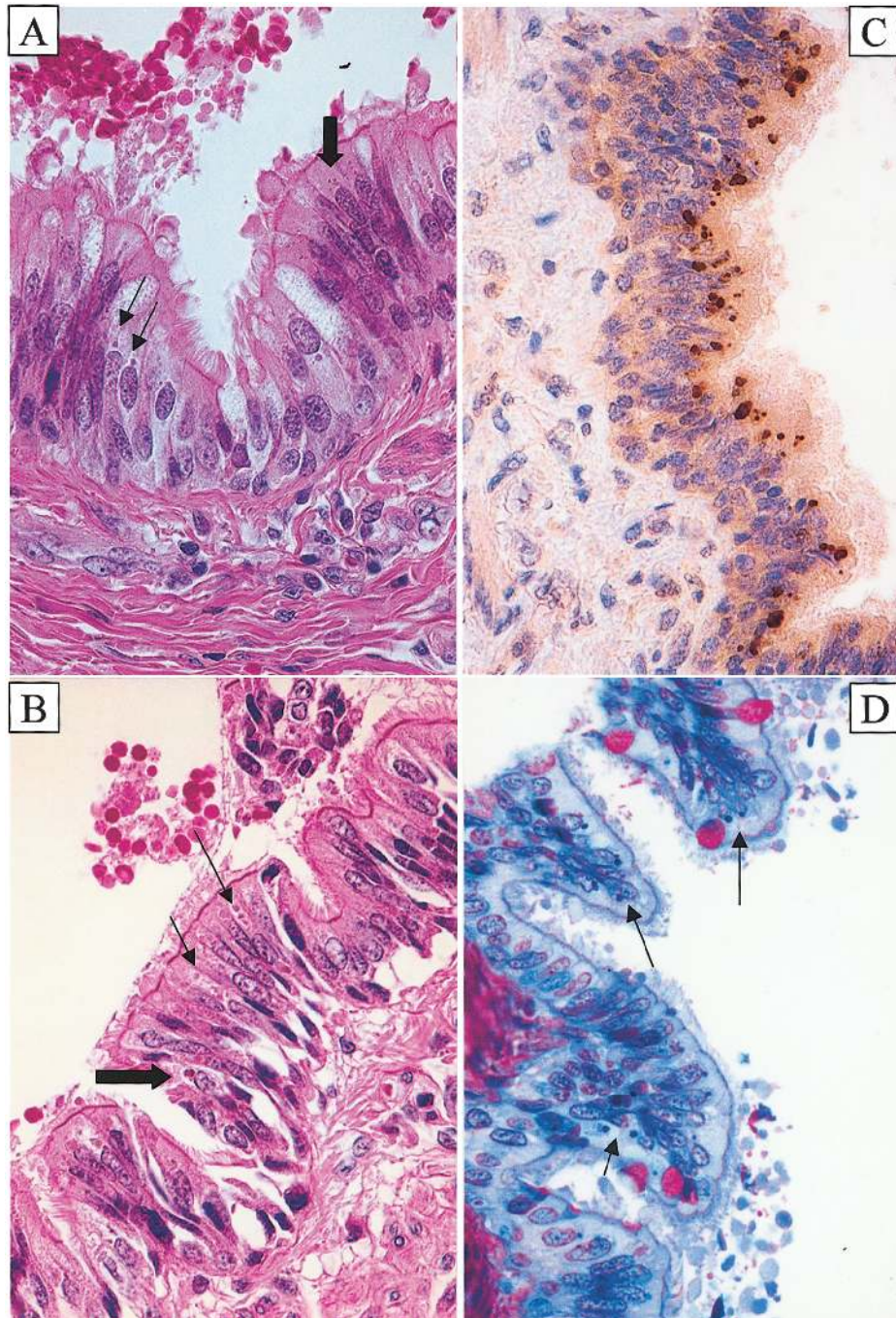


**Figure 1.** Cytoplasmic inclusion bodies are visible by light microscopy in acute Kawasaki disease (KD) ciliated bronchial epithelium. *A* and *B*, hematoxylin-eosin–stained sections from patients 4 and 6 showing amphophilic spheroidal cytoplasmic inclusion bodies (*thin arrows*) and irregular, golden yellow, granular, supranuclear pigment resembling classic lipofuscin (*thick arrows*). *C*, Immunohistochemistry–stained section from patient 3 demonstrating brown, spheroidal, cytoplasmic inclusion bodies identified with synthetic KD antibody J. *D*, Methylene blue/azure II/basic fuchsin trichrome–stained section from patient 2 showing dark blue cytoplasmic inclusion bodies; goblet cells stained red. Original magnifications,  $\times 640$  for all panels.

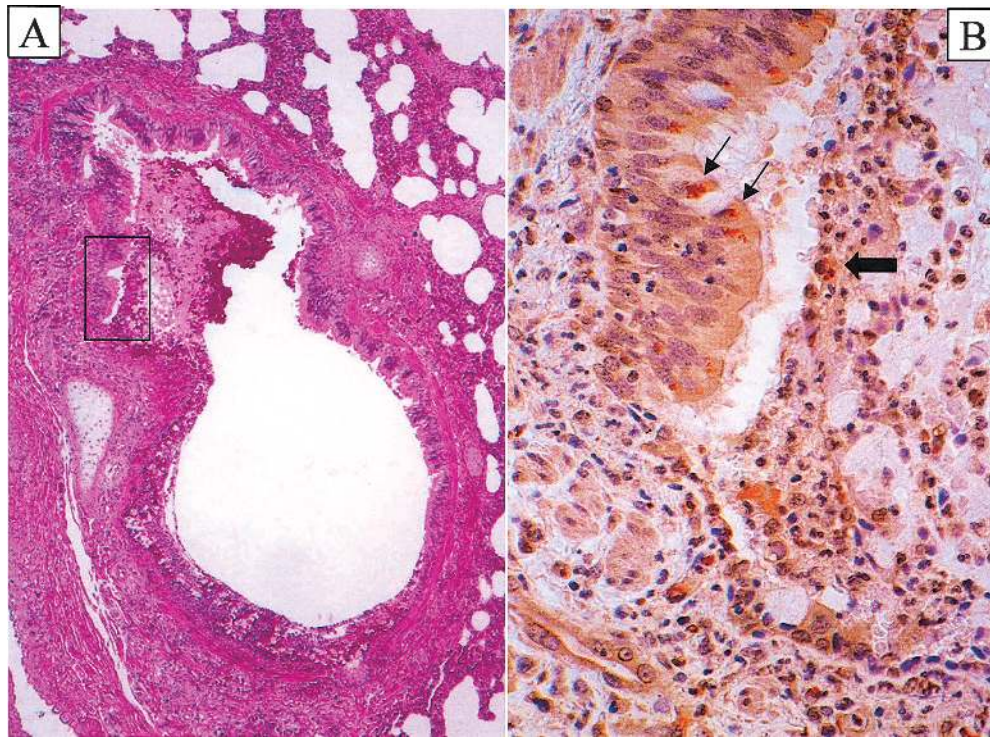


**Figure 2.** Detection of antigen in inflamed, partially necrotic bronchus from patient 4. *A*, Hematoxylin-eosin stain of bronchus. Most of the right side of the bronchus shows inflammation with intact epithelium; the bottom and most of the left side of the bronchus is devoid of epithelial cells, which have been replaced by an inflammatory exudate that spills over into the lumen. *B*, Immunohistochemistry-stained section, with synthetic Kawasaki disease antibody J, corresponding to the boxed area indicated in panel A. It demonstrates brown antigen in the remaining bronchial epithelial cells (*thin arrows*) and in the cytoplasm of a macrophage located in the adjacent inflammatory exudate (*thick arrow*). Original magnifications,  $\times 40$  for panel A and  $\times 640$  for panel B.

II/basic fuchsin trichrome stain (figure 1), indicating very concentrated protein and/or nucleic acid accumulation.

**TEM.** For patients 1–4, homogeneous, relatively regular, electron-dense inclusion bodies (up to 1.4 microns in diameter) were observed in the perinuclear region of the ciliated bronchial epithelial cells. Inclusion bodies were not present in nonciliated cells. These structures resembled the intracytoplasmic aggregates of viral proteins/nucleic acids, such as nucleocapsid aggregates, that are observed during infection with many RNA viruses (figures 3 and 4) [9–13]. Because membranes do not survive postmortem degeneration and the paraffin-embedding process, it was not possible to determine whether the inclusion bodies were membrane bound. Furthermore, these harsh conditions would undoubtedly obscure any ultrastructural features of virus-related structures that might be present in the inclusion bodies, for example, nucleocapsids and virions. Nothing resembling intranuclear inclusion bodies or viral components was identified in the nucleus. A section of the IHC-stained block face from patient 1 was compared with the TEM image from that area; excellent correlation was observed between the inclusion bodies identified by IHC and the electron-dense inclusion bodies observed by TEM (fig-

ure 3). In patients 1, 3, and 4, in addition to inclusion bodies, many smaller, pleomorphic, electron-dense bodies were also observed. These structures were mostly homogeneous, unlike typical lipofuscin. No structures resembling bacterial, fungal, or parasitic elements were observed by TEM in the inclusion bodies, the epithelial cells, or the ciliated border external to the cells from patients 1–4.

## DISCUSSION

In the present study, we report that LM and TEM demonstrate that synthetic KD antibodies A and J detect intracytoplasmic inclusion bodies in acute KD ciliated bronchial epithelial cells. The inclusion bodies are consistent with aggregates of viral proteins that are likely to be associated with nucleic acid. These results provide new insights into the etiology and pathogenesis of acute KD, and they suggest new directions for identification of the etiologic agent.

Although the coronary arteries are the most clinically significant site of inflammation in patients with acute KD, pathological studies indicate a high incidence of inflammatory lesions in many organs and tissues, including the lungs [14]. The epidemiologic

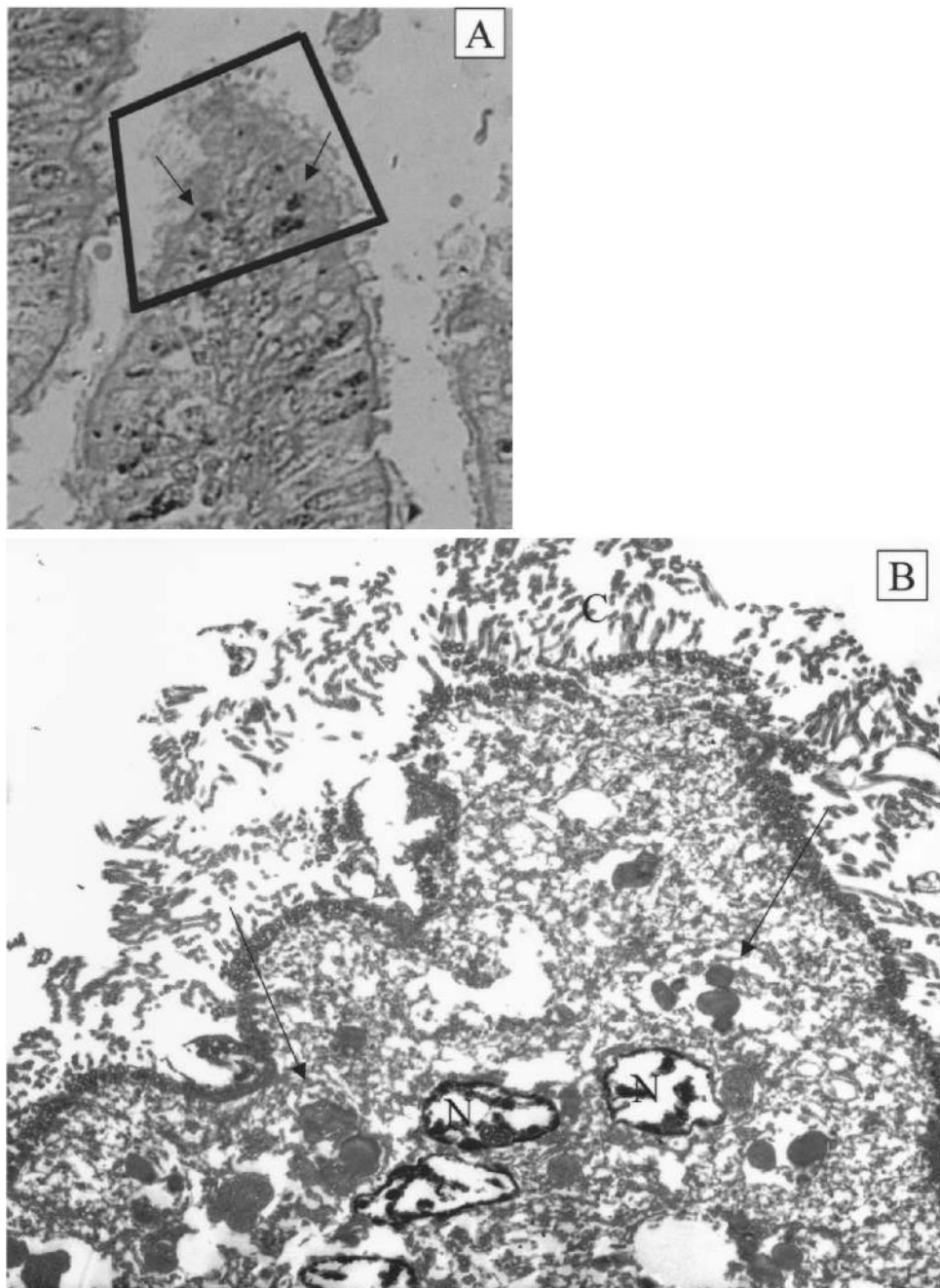


**Figure 3.** Correlation of cytoplasmic inclusion bodies as demonstrated by immunohistochemistry (IHC) and transmission electron microscopy (TEM). *A*, IHC block face from patient 1 demonstrating IHC-positive inclusion bodies (*arrows*). *B*, Homogeneous perinuclear inclusion bodies (*arrows*) demonstrated by TEM correspond to inclusion bodies demonstrated by IHC. The thickness of the TEM section is 0.08 microns, and the thickness of the IHC section is 5 microns; therefore, not all structures present in the IHC section can be observed in the TEM section. Original magnifications,  $\times 500$  for panel *A* and  $\times 2000$  for panel *B*. *C*, cilia; *N*, nucleus.

profile of KD supports a ubiquitous etiologic agent, and most ubiquitous infectious agents enter the body through either the respiratory or the gastrointestinal tract. The infiltration of IgA plasma cells into the upper respiratory tract in patients with acute KD occurs in a pattern similar to that generally observed during respiratory viral infections [4]. The predominance of CD8 T

lymphocytes in the inflammatory cell infiltrate during acute KD [5] implicates an intracellular pathogen as the etiologic agent. Our discovery that synthetic antibodies A and J bind to intracytoplasmic inclusion bodies in acute KD ciliated bronchial epithelium leads to speculation that the antibodies bind to antigens derived from the etiologic agent of KD and that the site of

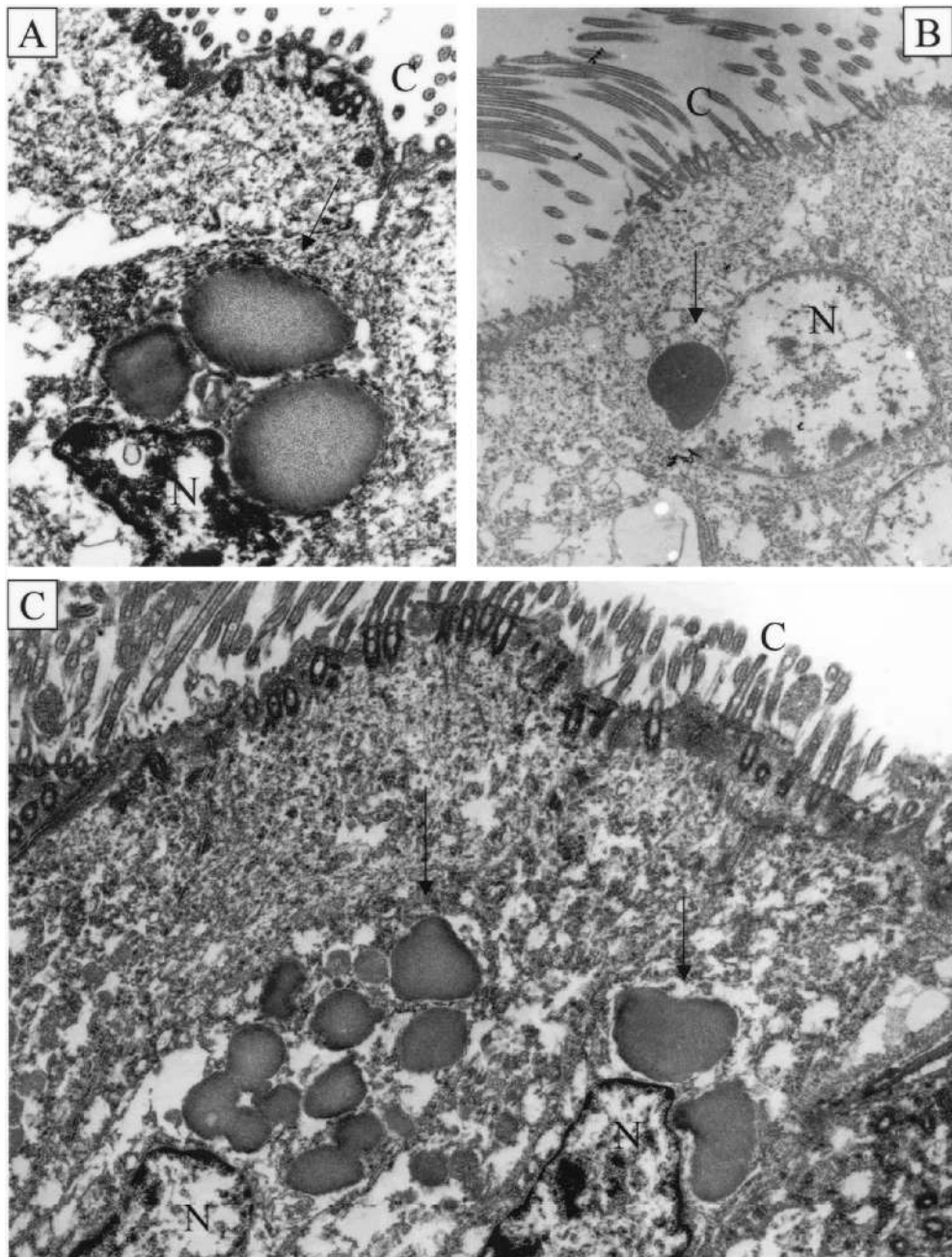


**Figure 4.** Homogeneous cytoplasmic perinuclear inclusion bodies observed by transmission electron microscopy in patients 2–4. *A*, Three regular, homogeneous perinuclear inclusion bodies (*arrow*) are observed in a ciliated bronchial epithelial cell from patient 3. *B*, A single homogeneous spheroidal inclusion body (*arrow*) is observed indenting the nucleus of a ciliated bronchial epithelial cell from patient 2. *C*, Multiple homogeneous bodies (*arrows*) are observed in ciliated bronchial epithelial cells from patient 4. Original magnifications,  $\times 17,000$  for panel A and  $\times 14,000$  for panels B and C. C, cilia; N, nucleus.

primary infection for acute KD may be the medium-sized bronchi of the lungs. Although limited TEM studies have been performed on lymph nodes, kidneys, conjunctivae, and peripheral blood from patients with acute KD [15–18], the lungs have not been examined. However, if the lungs are the site of primary infection for acute KD, examination of this tissue could be particularly important to understanding the disease’s pathogenesis.

Therefore, we studied ciliated bronchial epithelial cells from patients with acute KD by LM and TEM.

The normal ciliated bronchial epithelial cell is highly polarized, with an electron-dense nucleus and mostly electron-lucent cytoplasm. The rough endoplasmic reticulum and the Golgi complex are mostly apical and are adjacent to the nucleus. Small numbers of lysosomes can be present in the apical cy-



toplasm, and mitochondria are present close to the apical surface, to provide energy for the cilia. Inclusion bodies are observed in the apical cytoplasm of mammalian ciliated bronchial epithelial cells infected with RNA viruses, particularly those belonging to the *Paramyxoviridae* family [8]; these inclusion bodies represent aggregates of nucleocapsids.

Rapid, neutral-buffered glutaraldehyde fixation of fresh tissues is optimal for TEM, with rapid, neutral-buffered formalin fixation being second best. The tissue available to us from patients with acute KD was formalin fixed at autopsy and then embedded in paraffin and was, thus, exceedingly suboptimal for ultrastructural study. When TEM is performed on such material, cellular details such as membranes, cytoplasmic organelles, and infectious agents (especially viruses) are poorly preserved, at best. Although inclusion bodies consistent with aggregates of viral protein were observed in acute KD ciliated bronchial epithelial cells, viral particles or nucleocapsids were not identified, which, given the state of the tissue, does not rule out their presence.

Immune electron microscopy with gold beads is the optimal technique for confirming that the inclusion bodies observed by IHC are the same as the inclusion bodies observed by TEM; however, this technique is best suited to fresh tissues, which are virtually unavailable. Therefore, we aligned TEM images with the IHC-stained tissue block face and demonstrated that the inclusion bodies identified by the 2 techniques represented the same structures.

Inclusion bodies were predominantly observed in ciliated bronchial epithelial cells of medium-sized, compared with larger or smaller, bronchi. Recent evidence indicates that many respiratory viruses preferentially infect ciliated bronchial epithelial cells, potentially because they use certain sialic acid residues as receptors that are expressed only by ciliated epithelial cells [19, 20].

The detection of golden yellow, lipofuscin-like pigment in ciliated bronchial epithelium from some patients with acute KD was, at first, puzzling. Classic lipofuscin is an age-related pigment—it is especially seen in adult liver, brain, and heart—and consists of oxidatively modified cross-linked proteins originating from autophagocytized, indigestible cytoplasmic components [21]. Although accumulations of lipofuscin can be observed in the neurons of children with neuronal ceroid lipofuscinosis, we were unable to find a precedent for accumulations of lipofuscin-like material in tissues from otherwise healthy infants or even infants with other respiratory infections (such as RSV infection), particularly in bronchial epithelium. The lower quantity of pigment detected by Fontana stain, compared with that observed as golden yellow granular pigment detected by HE stain, and the relatively small pleomorphic brown bodies observed in the IHC preparations suggest that the pigment observed in HE-stained sections is not classic, age-related lipofuscin but rather may be pigment formed during a process of lysosomal degradation of

virus. Acute KD ciliated bronchial epithelium appears to contain large quantities of protein in inclusion bodies. The major cytoplasmic pathway used by eukaryotic cells to selectively degrade excess proteins is ubiquitin-dependent proteolysis in the proteasome. Proteins not degraded by proteasomes can be autophagocytized, further oxidized within lysosomes, and, therefore, partly converted into lipofuscin. It is possible that excessive viral protein produced in the bronchial epithelial cells cannot be handled by the proteasome and that, as a result, lysosomal activity is increased. Alternatively, several viruses—such as adenovirus [22], herpesviruses [23], and, potentially, severe acute respiratory syndrome coronavirus (CoV) [24]—may produce proteins that interfere with proteasome function to their advantage. Proteasome inhibition has been shown to enhance lipofuscin formation [25]. Thus, the etiologic agent of KD may interfere with proteasome function, resulting in increased lysosomal degradation of its proteins and resultant lipofuscin-like deposits containing undigested viral material.

Because synthetic antibodies A and J both bind to inclusion bodies in ciliated bronchial epithelial cells in patients with acute KD, and because both show binding to tissues from the same patients with acute KD, it is likely that these antibodies bind to the same or different epitopes of a single antigen. The detection of the inclusion bodies by synthetic monoclonal KD antibodies implies that KD results from infection with a single respiratory viral agent or a group of very closely related viral agents, as we suggested in our previous study [7]. A recent study reported detection of human CoV (HCoV) NL63 in respiratory samples from patients with acute KD by reverse-transcriptase polymerase chain reaction [26], but we, in collaboration with an international multicenter group of collaborators [27], and at least 2 other independent groups of investigators [28, 29] have subsequently tested respiratory samples from children with acute KD from diverse geographic locations and reported that acute KD is not associated with HCoV-NL63. Therefore, we believe that it is unlikely that the inclusion bodies we observed are the result of infection with HCoV-NL63.

We suspect that KD likely results from infection with an as yet unidentified viral agent. Identification of the antigen detected by use of synthetic KD antibodies A and J in acute KD tissues has been considerably hampered by the lack of fresh tissue samples available for analysis. Deaths from acute KD are rare but continue to occur worldwide. It will be critical to obtain glutaraldehyde-fixed tissue samples from future fatalities so that more-optimal ultrastructural experiments can be performed. Identification of the structure of any viral particles observed could be critical in narrowing the search for a viral etiologic agent. In the meantime, we are using various molecular methods to analyze formalin-fixed tissues in an effort to determine the nature of the viral proteins and/or nucleic acids present in the inclusion bodies.

## Acknowledgment

We acknowledge the excellent histological work of Leslie Kiefer.

## References

1. Rowley AH. Kawasaki syndrome. In: Gershon AA, Hotez PJ, Katz SL, eds. *Krugman's infectious diseases of children*. 11th edition. Philadelphia: Mosby, 2004:323–35.
2. Newburger JW, Takahashi M, Gerber MA, et al. Diagnosis, treatment, and long-term management of Kawasaki disease. *Circulation* 2004; 110:2747–71.
3. Rowley AH, Eckerley CA, Jack HM, Shulman ST, Baker SC. IgA plasma cells in vascular tissue of patients with Kawasaki syndrome. *J Immunol* 1997; 159:5946–55.
4. Rowley AH, Shulman ST, Mask CA, et al. IgA plasma cell infiltration of proximal respiratory tract, pancreas, kidney, and coronary artery in acute Kawasaki disease. *J Infect Dis* 2000; 182:1183–91.
5. Brown TJ, Crawford SE, Cornwall M, Garcia F, Shulman ST, Rowley AH. CD8 T cells and macrophages infiltrate coronary artery aneurysms in acute Kawasaki disease. *J Infect Dis* 2001; 184:940–3.
6. Rowley AH, Shulman ST, Spike BT, Mask CA, Baker SC. Oligoclonal IgA response in the vascular wall in acute Kawasaki disease. *J Immunol* 2001; 166:1334–43.
7. Rowley AH, Baker SC, Shulman ST, et al. Detection of antigen in bronchial epithelium and macrophages in acute Kawasaki disease by use of synthetic antibody. *J Infect Dis* 2004; 190:856–65.
8. *Paramyxoviridae*. In: Murphy FA, Gibbs EPJ, Horzinek MC, Studdert MJ, eds. *Veterinary virology*. 3rd edition. San Diego: Academic Press, 1999:411–28.
9. Bryson DG, McNulty MS, McCracken RM, Cush PF. Ultrastructural features of experimental parainfluenza type 3 virus pneumonia in calves. *J Comp Path* 1983; 93:397–414.
10. Goldsmith CS, Tatti KM, Ksiazek TG, et al. Ultrastructural characterization of SARS coronavirus. *Emerg Infect Dis* 2004; 10:320–6.
11. Gilka F, Spencer J. Viral matrix inclusion bodies in myocardium of lymphoid leukosis virus-infected chickens. *Am J Vet Res* 1985; 46: 1953–60.
12. Hyatt AD, Selleck PW. Ultrastructure of equine morbillivirus. *Virus Res* 1996; 43:1–15.
13. Wong KT, Shieh WJ, Kumar S, et al. Nipah virus infection: pathology and pathogenesis of an emerging paramyxoviral zoonosis. Nipah Virus Pathology Working Group. *Am J Pathol* 2002; 161:2153–67.
14. Amano S, Hazama F, Kubagawa H, Tasaka K, Haebara H, Hamashima Y. General pathology of Kawasaki disease. *Acta Pathol Jpn* 1980; 30: 681–94.
15. Giesker DW, Pastuszak WT, Forouhar FA, Krause PJ, Hine P. Lymph node biopsy for early diagnosis in Kawasaki disease. *Am J Surg Pathol* 1982; 6:493–501.
16. Bonany PJ, Bilkis MD, Gallo G, et al. Acute renal failure in typical Kawasaki disease. *Pediatr Nephrol* 2002; 17:329–31.
17. Burns JC, Wright JD, Newburger JW, et al. Conjunctival biopsy in patients with Kawasaki disease. *Pediatr Pathol Lab Med* 1995; 15: 547–53.
18. Koga M, Ishihara T, Takahashi M, Umezawa Y, Furukawa S. Activation of peripheral blood monocytes and macrophages in Kawasaki disease: ultrastructural and immunocytochemical investigation. *Pathol Int* 1998; 48:512–7.
19. Zhang L, Peebles ME, Boucher RC, Collins PL, Pickles RJ. Respiratory syncytial virus infection of human airway epithelial cells is polarized, specific to ciliated cells, and without obvious cytopathology. *J Virol* 2002; 76:5654–66.
20. Zhang L, Bukreyev A, Thompson CI, et al. Infection of ciliated cells by human parainfluenza virus type 3 in an in vitro model of human airway epithelium. *J Virol* 2005; 79:1113–24.
21. Terman A, Brunk UT. Lipofuscin: mechanisms of formation and increase with age. *Acta Pathol Microbiol Immunol Scand* 1998; 106: 265–76.
22. Balakirev MY, Jaquinod M, Haas AL, Chroboczek J. Deubiquitinating function of adenovirus proteinase. *J Virol* 2002; 76:6323–31.
23. Everett RD, Meredith MR, Orr A, Cross A, Kathoria M, Parkinson J. A novel ubiquitin-specific protease is dynamically associated with the PML nuclear domain and binds to a herpesvirus regulatory protein. *EMBO J* 1997; 16:1519–30.
24. Sulea T, Lindner HA, Purisima EO, Menard R. Deubiquitination, a new function of the severe acute respiratory syndrome coronavirus papain-like protease? *J Virol* 2005; 79:4550–1.
25. Terman A, Sandberg S. Proteasome inhibition enhances lipofuscin formation. *Ann NY Acad Sci* 2002; 973:309–12.
26. Esper F, Shapiro E, Weibel C, Ferguson D, Landry ML, Kahn JS. Association between a novel human coronavirus and Kawasaki disease. *J Infect Dis* 2005; 191:499–502.
27. Shimizu C, Shike H, Baker SC, et al. Human coronavirus NL63 is not detected in the respiratory tracts of children with acute Kawasaki disease. *J Infect Dis* 2005; 192:000–00 (in this issue).
28. Ebihara T, Endo R, Ma X, Ishiguro N, Kikuta H. Lack of association between New Haven coronavirus and Kawasaki disease (letter). *J Infect Dis* 2005; 192:351–2.
29. Belay ED, Erdman DD, Anderson LJ, et al. Kawasaki disease and human coronavirus (letter). *J Infect Dis* 2005; 192:352–3.